Applied Nanoscience (2020) 10:2057–2067
https://doi.org/10.1007/s13204-020-01355-5

ORIGINAL ARTICLE

Understanding the potential of bio-fabricated non-oxidative silver nanoparticles to eradicate *Leishmania* and plant bacterial pathogens

Bilal Javed[1,2] · Naveed Iqbal Raja[2] · Akhtar Nadhman[3] · Zia-ur-Rehman Mashwani[2]

Received: 7 February 2020 / Accepted: 11 March 2020 / Published online: 28 March 2020
© King Abdulaziz City for Science and Technology 2020

Abstract

The present study was aimed to use an aqueous extract of *Mentha arvensis* L. to bio-fabricate silver nanoparticles (AgNPs) and evaluation of the potential of non-oxidative nanoparticles in photodynamic treatment of pathogens. Spectrophotometric analysis of colloidal AgNPs represented a characteristic SPR band at 485 nm of the light wavelength. Nanoparticles were structurally anisotropic and nearly spherical and observed between ~ 20 and 100 nm by using SEM and AFM images. The dynamic light scattering technique determined particle size between ~ 14 and 32 nm. Biological applications manifested that the AgNPs are highly biocompatible and caused rupturing of RBCs at an exceptionally high dose estimated as ~ 214 µg/ml, while 10 µg/ml of AgNPs killed nearly ~ 50% of *Leishmania tropica*. AgNPs were also found effective to curb the growth of various plant bacterial pathogens and the dose-dependent response was observed in between ~ 2 and 12 µg/ml and MIC was recorded at 12 µg/ml. ROS quantification revealed that the AgNPs are not potent to produce free radicles and did not report any quantum yield. The elemental composition analysis of AgNPs by EDX confirmed that these nanoparticles are non-oxidative. ROS quantification and photothermal activity evaluation showed that these nanoparticles cannot be used in photodynamic therapy. The experimental outcomes of this study clarify the use of biocompatible AgNPs into pharmaceutical formulations to treat Leishmaniasis and plant bacterial pathogens.

Keywords Anti-leishmanial · Biocompatible · Green synthesis · Microbial resistance · *Mentha arvensis* · Photodynamic

Introduction

Bio-fabrication of silver nanoparticles by harnessing the natural abilities of the plant secondary metabolites provide a one-step process that not only converts the bulk material into their nano-forms by redox chemical reactions but also contributes to shield metallic nanocore by covering the surface with functional groups found primarily in plant body (Sharma et al. 2009; Manosalva et al. 2019). Nanoparticles of silver, because of their unique size, shape and structure have abilities to interact with the plasma cell membrane and control the proliferation of the organisms (Siddiqui et al. 2018; Khatami et al. 2018; Behravan et al. 2019).

Leishmaniasis is a disease of an intracellular parasite spread by the bites of a phlebotomine sand-fly. This disease is usually caused by a protozoan belongs to a Genus *Leishmania* and causes acute to chronic ailments that range from cutaneous ulcers to mutilating mucocutaneous disease and sometimes it causes severe systematic illnesses to the infected persons (Nadhman et al. 2014). The conventional treatment of *Leishmania* involves the use of different inhibitory drugs but the microorganism attains resistance after some time and results in the more severe action or attack of disease which makes it difficult to control (Iqbal et al. 2019b). The use of nanoparticles plays a very important role to kill microorganisms without allowing them to develop resistance (Abbasi et al. 2019).

Multiple drug resistance is another issue that deals with the abilities of microorganisms to attain resistance against

✉ Bilal Javed
javedbilal87@gmail.com; javedb@sas.upenn.edu

✉ Zia-ur-Rehman Mashwani
zia.botany@gmail.com; mashwani@uaar.edu.pk

[1] Roy and Diana Vagelos Laboratories, Department of Chemistry, University of Pennsylvania, Philadelphia, PA 19104-6323, USA

[2] Department of Botany, PMAS-Arid Agriculture University, Rawalpindi 46300, Punjab, Pakistan

[3] Institute of Integrative Biosciences, Department of Biotechnology, CECOS University, Peshawar, Pakistan

modern drugs due to drug abuse and poor management (Pareek et al. 2018; Alavi et al. 2019). Drug resistance is reckoned as a leading cause of mortality and morbidity in the coming decade and will be effecting organisms more severely than ever before (Rai et al. 2017). *Xanthomonas oryzae* is a Gram-negative bacterial strain and is responsible to cause a bacterial blight on rice plants. This is a major problem in tropical Asia where high yield rice crops are mainly infected by this bacterium. It causes vascular disease and grows in the form of lesions of white or grey color along with the veins of a leaf (Bai et al. 2000). *Xanthomonas vesicatoria* is a rod-shaped Gram-negative bacterium that is responsible to cause bacterial spots on the leaves of tomato and pepper plants. After getting infected with this bacterium the symptoms become visible on the above-ground plant parts such as on stem canker, fruit and the leaves spots become easily visible (Ciardi et al. 2000). *Ralstonia solanacearum* is a Gram-negative anaerobic pathogenic bacterium that has a wide range of plant hosts and mostly colonizes in the xylem of the plant body to cause bacterial wilt. It affects potato, tomato, olive, banana, ginger, soya bean, rose, and tobacco plants (Champoiseau et al. 2009). *Erwinia carotovora* is also a Gram-negative rod-shaped bacterium that was first identified from the carrot plant. It is responsible to cause infections to a variety of plants including carrots, lettuces, potatoes, cucumbers, onions, tomatoes, and many ornamental plants. It infects the plant tissues both in situ and in storage. It results in the softening of the plant tissues and makes them watery and slimy and causes fouling smell (Dong et al. 2004).

The surface covering of nanoparticles has functional groups that originate from secondary metabolites and provide various attributes and underpin their suitability for photodynamic applications. Photodynamic mobilization of a drug depends on its photooxidative and photothermal potentialities (He et al. 2020). Photodynamic therapy plays a very important role to manipulate the electromagnetic and kinetic potential of nanoparticles by exciting them on a suitable wavelength usually at visible and infrared light which helps to release reactive oxygen species (ROS) usually singlet oxygen ($^1O_2$) and other ROS (Beik et al. 2019). The release of free electrons results in the disruption of cells homeostasis and osmotic potential by kinetic movement and ionic balance by unregulated ion flow and eventually leads to cell death (Lamch et al. 2018). The development of new photo-nanodynamic drugs provides the most modern platform to the researchers to combat the war of proliferating vicious pathogens.

Herein we report (detailed layout of the study is represented in Scheme 1) the use of Ag nanoparticles of different shapes, sizes, and morphologies, phytosynthesized from *Mentha arvensis* to eradicate *Leishmania* and plant bacterial pathogens and determination of their photodynamic potential.

Materials and methods

Processing of plant material

Mentha arvensis has purchased from the local farmers market Sialkot (32.485272° N 74.543575° E) Pakistan. Samples were washed, dried to remove the moisture, chopped into small pieces and pulverized in the kitchen grinding machine to make a fine powder. For the preparation of aqueous extracts 1 to 10 ratio of plant material and distilled water was prepared respectively and heated on a hot plate at 45–65 °C for 10–20 min. After the boiling, the aqueous extract was filtered and used immediately as fresh for the reduction of silver salt (Alshehri et al. 2019).

Chemical reagents

The chemical reagents purchased for the synthesis of silver nanoparticles were of analytic grade and used as received without any further purification.

Synthesis of silver nanoparticles

Silver nitrate solution of 5 mM concentration was mixed with freshly prepared plant extract in a ratio of 1:9 of plant extract and $AgNO_3$ solution respectively. The reaction was carried out at 5.88 pH, the temperature was maintained at 60 °C and the reaction mixture was stirred continuously. An aliquot was taken out from the flask and the absorbance was measured by using crystalline Quartz cuvettes with the help of UV–visible spectrophotometer (Shimadzu 1601, Japan) in the range of 200–900 nm of the wavelength of light. Absorbance was measured after a specified interval of time to observe the reaction kinetics at different incubation periods to determine the synthesis and the yield of AgNPs. After the completion, the reaction was quenched by removing the flask from the hot plate and diluted with a small amount of distilled water. The reaction mixture was centrifuged at 1000×*g* (Sorvall RT 7 Plus) for 1 h, washed with methanol and distilled water thrice to separate the AgNPs from the reaction mixture (Akhtar et al. 2013; Ali et al. 2016; Kim et al. 2016).

Morphological characterization

Characterization of synthesized silver nanoparticles was performed by using different material characterization techniques to explore their morphologies. Characterization was done initially by visual observation that involves the comparison of reaction mixture before and after synthesis. UV–visible Spectrophotometer (Shimadzu 1601, Japan) was used to measure the absorbance of the reaction mixture at various intervals of incubation to confirm the highest yield and synthesis (Huang et al. 2019). Scanning Electron Microscope (SEM) JEOL 7500F HRSEM, was used to get a mean size and shape of nanoparticles by observing the sample placed on copper grids under different lens and voltages of a microscope (Thirumagal and Jeyakumari 2019). Energy-dispersive X-ray analysis (EDX) was performed to check the elemental composition of the sample by using detectors associated with JEOL 7500F HRSEM (Alsammarraie et al. 2018). Atomic Force Microscopy (AFM) images were collected on Agilent 5500 AFM and the sample was placed on a silicon wafer and was prepared on a spin coater machine (Laurell WS-650Mz-23NPP) to spread AgNPs (Li et al. 2019). The hydrodynamic diameter of NPs was measured by using the dynamic light scattering (DLS) machine of Malvern Instruments particle sizer, Zetasizer Nano S, Malvern Instruments, UK. The sample was prepared into 1× PBS solution and 1 ml of solution was observed at 25 °C by using laser and other reaction parameters were adjusted automatically by automatic machine settings (Satsangi 2019).

Biocompatibility assessment (Hemolysis Assay)

The biocompatibility of AgNPs was studied by using the hemolytic assay. Human fresh red blood cells (RBCs) (collected after oral consent and approval by University Bioethical Committee) were washed several times by using Hank's Buffer Salt Solution (HBSS). After the washing of the RBCs, the 180 µl of RBCs suspension (in HBSS 4% Volume) was placed in 96-well plate and AgNPs were prepared in different doses and introduced to RBCs. After that plates were incubated for 3 h in 5% CO_2 chamber and the temperature was maintained at 37 °C. The cell suspension was taken in Eppendorf tubes and centrifuged at 1000×*g* for 5 min. The release of the hemoglobin pigment by the ruptured RBCs was measured at 576 nm of the wavelength of the light by taking the supernatant from 96-well plate and measured by using a microplate reader (Thermo Fisher). Negative control was maintained by using RBCs in HBSS without AgNPs while the positive control was maintained by using Triton X-100 (0.1%). Percentage hemolysis was determined by using the following formula. Lethality dose (LD_{50}, LD_{90}, and LD_{100}) was recorded by using GraphPad Prism® software and plotted into a graph (Nadhman et al. 2015; Iqbal et al. 2019a);

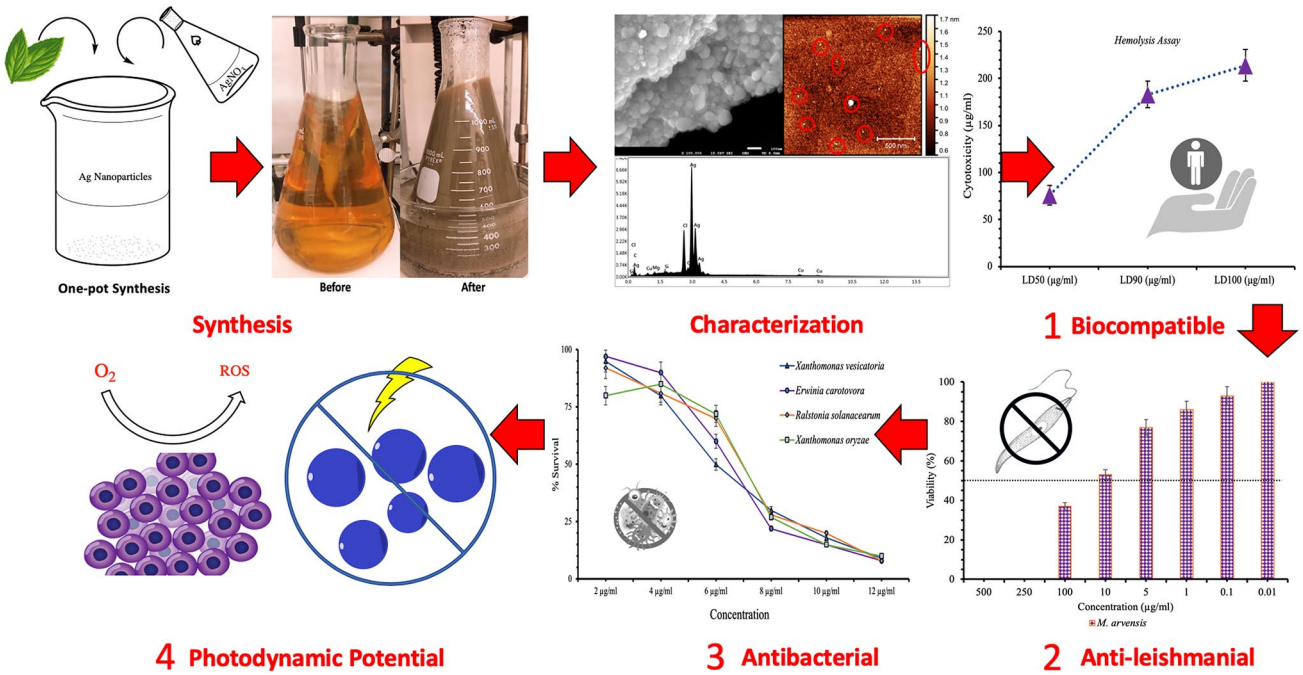

Scheme 1 Schematic layout of the work

$$\text{Hemolysis}\ (\%) = \frac{\text{OD at } 576\text{ nm in the nanoparticle solution} - \text{OD at } 576\text{ nm in HBBS}}{\text{OD at 576 nm in } 0.1\%\text{ Triton X} - 100 - \text{OD at } 576\text{ nm in HBBS}} \times 100$$

L. tropica culture maintenance

Leishmania tropica (KWH23) were maintained on medium 199 (M199) (Gibco, Invitrogen, USA). The medium was supplemented with 10% heat-inactivated fetal bovine serum (PAA, Austria), 100 mg/ml of streptomycin and 100 µg/ml of penicillin (Sigma, USA) (Nadhman et al. 2014, 2015).

Anti-Leishmania activity measurement

A stock solution of AgNPs (1 mg/ml) was prepared in deionized water. *L. tropica* were grown in M199 medium for 7 days at 24 °C. *L. tropica* cells were suspended into 96-well microtiter plate and the serial dilution of AgNPs were prepared (500 µg/ml, 250 µg/ml, 100 µg/ml, 10 µg/ml, 5 µg/ml, 1 µg/ml, 0.1 µg/ml and 0.01 µg/ml). Cells viability was measured by doing counting on the Neubauer chamber (Thermo Fisher) by observing their motility with trypan blue die. IC_{50} was measured by using GraphPad Prism® Software (Nadhman et al. 2014, 2015; Iqbal et al. 2019a).

Antimicrobial activity evaluation against plant bacterial pathogens

All bacterial plant pathogens (*Erwinia carotovora, Xanthomonas vesicatoria, Xanthomonas oryzae* and *Ralstonia solanacearum*) (Plant Pathology Department, Agriculture University, Peshawar) (Naz et al. 2020) were grown overnight in Luria Bertani liquid media (tryptone = 10 g, yeast extract = 5 g and NaCl = 10 g in 1 L of distilled water; pH 7.2) and 1×10^8 cells/ml were maintained. Cells were plated into 96-well microtiter plates. Different concentrations of the AgNPs 500 µg/ml, 250 µg/ml, 100 µg/ml, 10 µg/ml, 1 µg/ml, 0.1 µg/ml, and 0.01 µg/ml were prepared and introduced to their receptive wells on the plate. Plates were incubated for 24 h at 37 °C on a rotatory shaker. After 24 h plates were read by measuring the absorbance at 600 nm of a microplate reader (Thermo Fisher, USA). The data were expressed in the form of % survival of bacterial pathogens against different nanoparticle concentrations (Nadhman et al. 2015).

ROS quantification

ROS generation by AgNPs was measured by preparing the DPBF solution (0.1 mM DPBF in ethanol). 10 µg/ml of AgNPs were dissolved into 2 ml of DPBF solution. The reaction was carried out into sealed Quartz cuvettes with IR filter (400–800 nm) for 30 s under sunlight. After each 30 s photobleaching of the DPBF was measured by using UV-3000 Spectrophotometer for 5 min. Methylene blue was used as a control (Nadhman et al. 2014, 2015).

Photothermal activity measurement

AgNPs were suspended into distilled water at a concentration of 1 mg/ml. The test tube containing the test sample was exposed to sunlight and after each minute temperature of the sample was recorded by dipping the temperature prob (Thermo scientific, USA). This procedure was continued for 30 min and a plot was drawn in-between time and temperature changed (Iqbal et al. 2019a).

Data analysis

All the experiments in this study were performed in triplicate and were expressed in the form of mean and standard deviation. MS Excel® was used to plot graphs and figures. Fiji image J® was used for the arrangement of microscopic images. *T* test was performed to analyze statistical differences in the results of antimicrobial, anti-leishmanial activity, photothermal activity and hemolysis assays and $P < 0.05$ was used to indicate significant difference.

Results

Phyto synthesis of AgNPs

Ag nanoparticles were synthesized by modulation of physicochemical parameters such as temperature, pH, the concentration of $AgNO_3$, concentration of plant extract and the ratio of reactants in our lab previously. It was confirmed that the physicochemical toolbox plays a very important role to steer the process of AgNPs synthesis and affects greatly the size, shape and biological corona of AgNPs that can change their biomedical nature (Beddoes et al. 2015). It was observed that the 5 mM of $AgNO_3$ at 60 °C and pH of the reactants after mixing were maintained at 5.88 appeared as optimum conditions for the synthesis of AgNPs by mixing plant aqueous extract and silver salt in 1 to 9 ratios respectively (Fig. 1 inset). UV–visible spectrums showed

the characteristic surface plasmon resonance (SPR) band at 485 nm in between 350 and 650 nm of the light wavelength (Fig. 1).

Physical characterization of AgNPs

The morphological characterization of AgNPs synthesized by the plant-mediated eco-friendly method was performed mainly by using SEM and AFM. SEM micrographs showed that NPs are spherical and have a size range of ~ 20–100 nm (Fig. 2a, b) which was further confirmed by using AFM images. AFM reported NPs of very small sizes and most of the NPs were found to be in a range of ~ 10–100 nm. AFM images again explained that the NPs are spherical (Fig. 3). The elemental composition of AgNPs was obtained by using EDX analysis (Fig. 2c). The characteristic peak of the Ag has observed at 3 keV and the intensity of the Ag signal was ~ 81%. No elemental O_2 was reported which showed that these nanoparticles are non-oxidative. It also reported the presence of C, Cl, Si, Mg, and Cu as 2.87%, 11.75%, 0.87%, 0.38%, and 3.62% respectively in trace amount. DLS analysis determined the particle size distribution and it was found between ~ 14 and 32 nm which represents the size range of most of the colloidal nanoparticles (Fig. 4) while the average size of a single nanoparticle was recorded at 20.46 nm. Polydispersity index was recorded as 0.220 which explains that these nanoparticles are monodisperse and are very suitable for biomedical applications.

Biocompatibility measurement of AgNPs (hemolysis)

Hemolysis assay provides a preliminary base to determine the biocompatibility of NPs. Hemolysis assay results were measured in terms of Lethal Dose (LD). LD_{50}, LD_{90}, and LD_{100} (Fig. 5) showed that a very high dose of the AgNPs is required to cause toxicity against human RBCs. 214 µg/ml was reported to be a lethal dose to kill 100% population of the test samples while a very minimal dose of the AgNPs (10 µg/ml) was found effective against *L. tropica*. LD_{50} and LD_{90} were recorded as 76 µg/ml and 184 µg/ml respectively which manifested a dose-responsive activity of AgNPs ($P < 0.05$).

Measurement of the dose-dependent response of the AgNPs against *Leishmania tropica*

Leishmaniasis is a disease which is caused by the bites of Phlebotomine sand-fly. Around 700,000 to 1 million new cases and some 26,000–65,000 deaths are reported annually by Leishmaniasis (WHO) (Iqbal et al. 2019b). AgNPs expressed a significant dose-dependent response against *Leishmania* ($P < 0.05$) and it was found that increasing the dose of AgNPs has more strong effects on the growth or the viability of *Leishmania* (Fig. 6). IC_{50} measurement showed that the 13.1 µg/ml of AgNPs dose is required to affect the growth of protozoans. It was observed that the 500 µg/ml of AgNPs killed 100% cells and the viability increased by decreasing the concentration of AgNPs ($P < 0.05$). Almost 50% of the population of the *Leishmania* found dead by using 10 µg/ml of AgNPs which is showing that these NPs are highly biocompatible as a very high dosage is required to affect the growth or to cause cytotoxicity to RBCs.

Measurement of the dose-dependent response of the AgNPs against plant bacterial pathogens

The dose-dependent activities of AgNPs were measured against *E. carotovora, X. vesicatoria, X. oryzae* and *R. solanacearum*. AgNPs were found to be highly effective against all pathogens and manifested dose-dependent responses (Fig. 7). As the concentration of the AgNPs dose decreased from 500 µg/ml, 250 µg/ml, 100 µg/ml, 10 µg/ml, 1 µg/ml, 0.1 µg/ml to 0.01 µg/ml, survival % of the bacterial pathogens increased significantly ($P < 0.05$). AgNPs manifested the MIC around 12 µg/ml against all pathogens which shows the potential of these nanomoieties to may act as a pesticide against plant disease-causing pathogens. The dose-dependent responses of bacterial pathogens were recorded in between 2 and 12 µg/ml. Ampicillin was used as a positive control and water was used as a negative control. The highest inhibition of pathogens at 10 µg/ml of ampicillin dose was 90%, 68.2%, 72% and 71.79% against *X. vesicatoria, E. carotovora, R. solanacearum*, and *X. oryzae* respectively. This inhibitory effect of AgNPs is because of the unique physical and chemical characteristics that provide them with abilities to enter bacterial cytoplasm by crossing plasma cell membrane barriers and to kill them eventually by disruption of ionic balance and rupturing membrane (Du et al. 2018).

ROS quantification of AgNPs

The generation of free radicals plays a very important role to increase the cytotoxic abilities of nano-antibiotic drugs. ROS scavenge the ionic potential of the cells and disturb the osmotic balance which results in the disruption of the plasma cell membrane and the death of the cell. Our AgNPs expressed zero quantum yield.

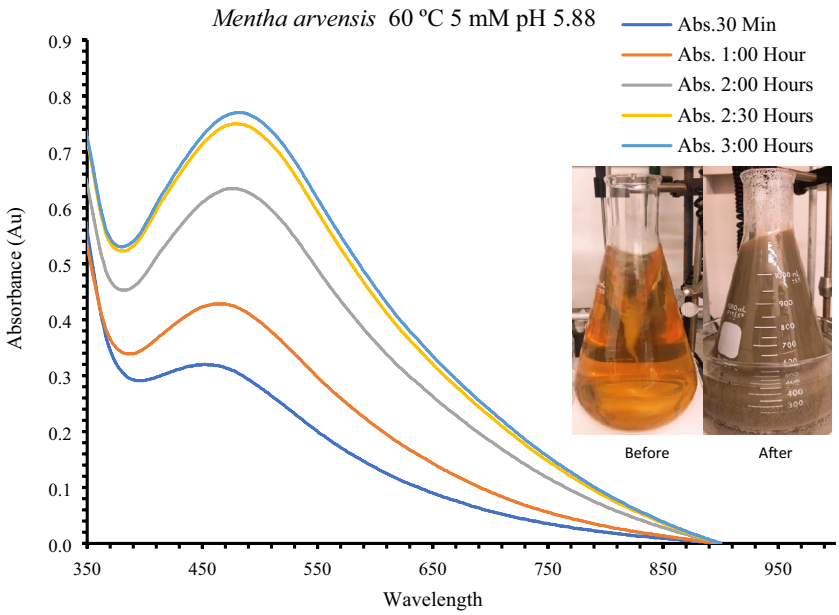

Fig. 1 UV–visible spectrum representing the time-dependent synthesis of AgNPs. Inset is showing a change in the color of the reaction mixture after the synthesis of AgNPs

Photo-thermal activity determination of AgNPs

Photo-thermal activity measurement did not report any change in temperature of AgNPs and the temperature remained constant even after 30 min (Fig. 8). Change in temperature of the NPs containing sample is reported if NPs have O_2 in them. Change in temperature also plays a very important role to use NPs as a photodynamic agent to treat dreading diseases including cancer and *Leishmania*. So, the results of our study showed that AgNPs synthesized from *M. arvensis* cannot be used as a photodynamic agent in the photothermal treatment of ailments.

Discussion

Specialized mechanisms that are responsible for developing antimicrobial resistance include drug/antibiotic selective pressure, housekeeping genes that code for the proteins or transporters to expel the antimicrobial drug out of the bacterial cell and results in decreasing the dose and have effects on the bacterial population, enzymatic inhibition of drugs and chemical modification of targeted sites leads to the development of multiple drug-resistant (MDR) organisms (Rai et al. 2017). So the present study involves the use of sustainable non-oxidative silver nanoparticles to treat microbial proliferations. Biogenic synthesis of AgNPs provides advantages to manufacture biocompatible nanodrugs for human applications. Plant bodies have various secondary metabolites that vary among species to species and sometimes the same plant species have different concentrations and constituents of phytometabolites due to spatial and temporal variations (Gobbo-Neto et al. 2017). The use of a 1 to 9 ratio of plant extract and silver salt reported the consumption of a very meager amount of secondary metabolites to reduce and stabilize AgNPs which guarantee reproducibility. Change in the color of the reaction mixture which is attributed to the response of AgNPs to light was observed initially to report synthesis (Fig. 1 inset). Surface plasmon resonance (SPR) band which is a result of the vibration of free electrons of AgNPs in coordination with the metal lattice in resonance and the oscillating electromagnetic field of light waves, was observed at 485 nm (Nindawat and Agrawal 2019). An increase in the incubation period of reactants resulted in increasing the absorbance at a higher wavelength which is called Redshift (460–485 nm, Fig. 1). According to Mie's theory, small molecules absorb light at a smaller wavelength while large molecules absorb light at a longer wavelength (Ulaeto et al. 2019). The microscopic structural evaluation showed that AgNPs are spherical and monodisperse and exist between ~ 20 and 100 nm. Particle size analysis manifested that most of the NPs are in the range of ~ 14–32 nm which is showing that the nanoparticles are very small in size and the narrow dispersity was recorded (PDI 0.220) which shows that the NPs are suitable for biomedical applications.

Biocompatibility is the main feature that contributes toward the application of NPs on different life forms, which was confirmed by using hemolysis assay (Jadhav et al. 2018). Blood is the main connective tissue in the human's and the animal's body. It supplies and exchange nutrients, maintain pH, transport hormones, deliver oxygen, transfer biochemical signals, immune response, defense mechanisms, maintain homeostasis and also act as a site for many biochemical reactions (Iqbal et al. 2019b; Parthiban et al. 2019). Figure 5 manifested the biocompatibility results of AgNPs.

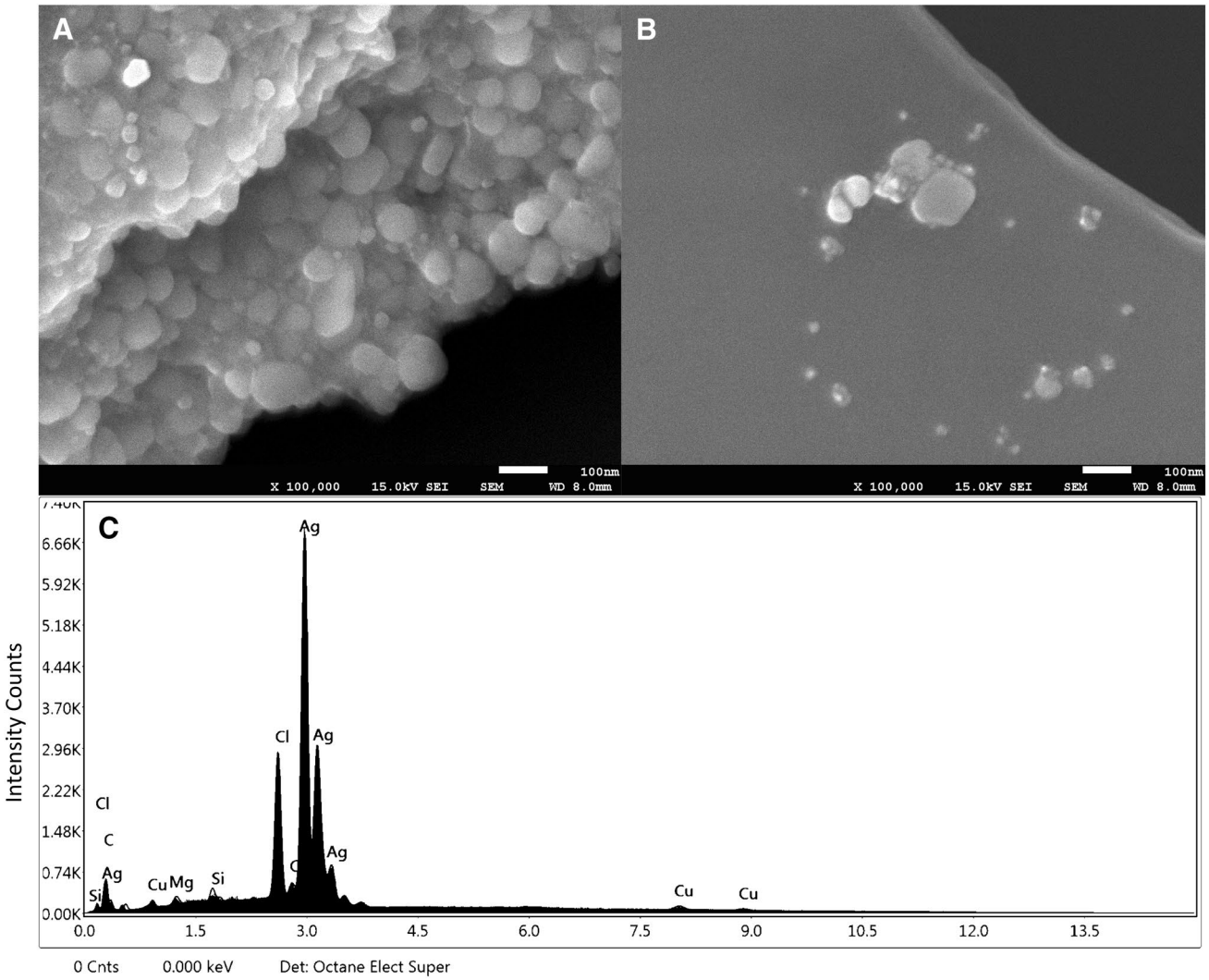

Fig. 2 **a**, **b** SEM micrographs representing that the AgNPs are spherical and have a size range of ~ 20–100 nm **c** EDX analysis of the AgNPs representing a peak of Ag at a characteristic region of 3.0 keV

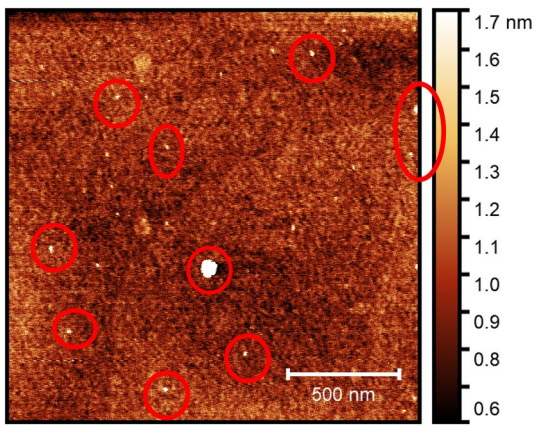

Fig. 3 AFM micrographs of AgNPs. Nanoparticles in Red circles are showing that they are spherical and have a size range of ~ 10–100 nm

Biological applications of the NPs implicated in this study found that the NPs are highly biocompatible and a single dose of 10 µg/ml of NPs is enough to eradicate almost 50% of the *Leishmania* population. AgNPs were observed biocompatible at a lower dose and increasing dose induced the rupturing of RBCs. The selective activity of AgNPs against *Leishmania* cells can be because of the presence of chlorides in colloidal AgNPs. Chlorides contribute to exchange bicarbonates (HCO_3^-) across the plasma cell membrane of the RBCs or erythrocytes and help to maintain ionic balance which is termed as chloride shift. The chloride ions form strong acids upon reaction to the water which may result in the antimicrobial activities against *Leishmania* and plant bacterial pathogens (Westen and Prange 2003). The biocompatibility of the AgNPs depends on the method of the synthesis and the surface modifications of the NPs. Surface functional groups play an important role to shield

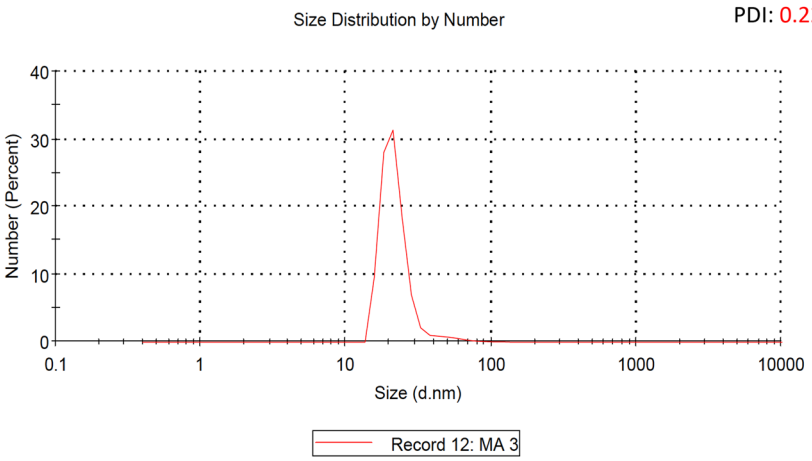

Fig. 4 Size distribution of AgNPs measured by using DLS analysis. Size distribution by number was observed between ~ 14 and 32 nm while the average size of a single nanoparticle was recorded as 20.46 nm. Polydispersity was recorded as 0.220

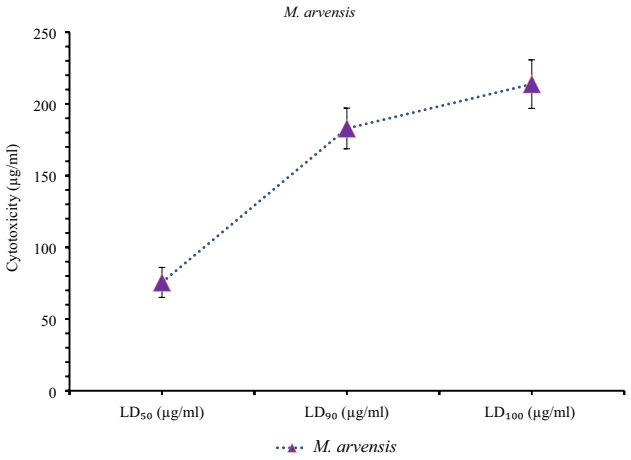

Fig. 5 Biocompatibility Measurement. LD_{50}, LD_{90} and LD_{100} of AgNPs. Increasing lethal dose resulted in increased cytotoxicity of AgNPs against RBCs

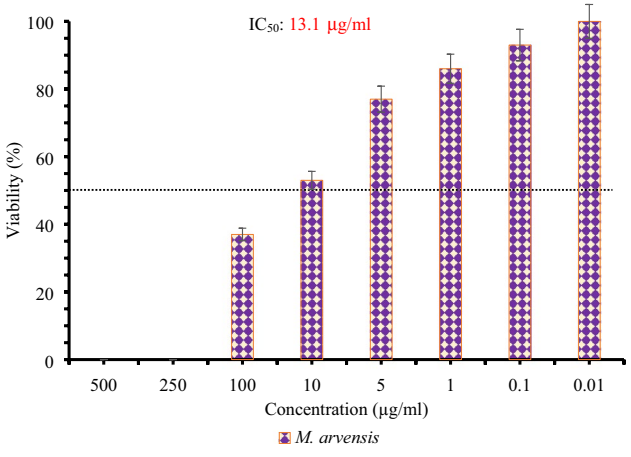

Fig. 6 Anti-leishmanial activity of different doses of silver nanoparticles represents the dose-responsive activity. Increasing the dose of silver nanoparticles resulted in decreasing viability percentage

the metallic core of AgNPs and belong to plant secondary metabolites originally that prevent the agglomeration of NPs and make them compatible for humans and other animals (Akhtar et al. 2013).

The dose-responsive activity was observed against *Leishmania tropica* and plant bacterial pathogens such as *Erwinia carotovora, Xanthomonas vesicatoria, Xanthomonas oryzae*, and *Ralstonia solanacearum*. It was observed that increasing the dose of the drug resulted in increasing the drug pressure on microorganisms, which promoted the process of killing (Sharma et al. 2009). At a higher dose 500 µg/ml and 250 µg/ml, there was no active growth of *Leishmania* parasite responsible to cause Leishmaniasis but the viability of the organisms increased with decreasing the dose while 10 µg/ml was found effective to kill more than 50% of the test population which is a great number. Plant bacterial pathogens were found highly susceptible against AgNPs and antimicrobial activity was recorded between 2 and 12 µg/ml and MIC was observed as 12 µg/ml. Our results are in favor of some previously published scientific reports (Jemilugba et al. 2019; Behravan et al. 2019; Anandan et al. 2019). Elemental composition analysis confirmed the presence of Cl (11.75%) in AgNPs. Chlorine-containing sesquiterpenes and monoterpene can be responsible for the presence of Cl (Dembitsky 2002; Shaiq Ali et al. 2002). Some previous reports established the antimicrobial potential of Cl (Odlaug 1981; Gottardi and Nagl 2005; Kim et al. 2008) and the presence of high chlorine contents in *M. arvensis* fabricated AgNPs can be one reason for their selective antimicrobial activities. Other factors responsible for the antimicrobial potential of AgNPs against *Leishmania* and plant bacterial pathogens can be a small size that helps nanoparticles to pass the plasma cell membrane barrier and enter the cytoplasm and fragment the DNA structure. Nanoparticles also have abilities to disrupt the ionic potential of cell membrane (Jadhav et al. 2018), bind with the thiol group (–SH) of respiratory enzyme's active sites (Behravan et al. 2019) and

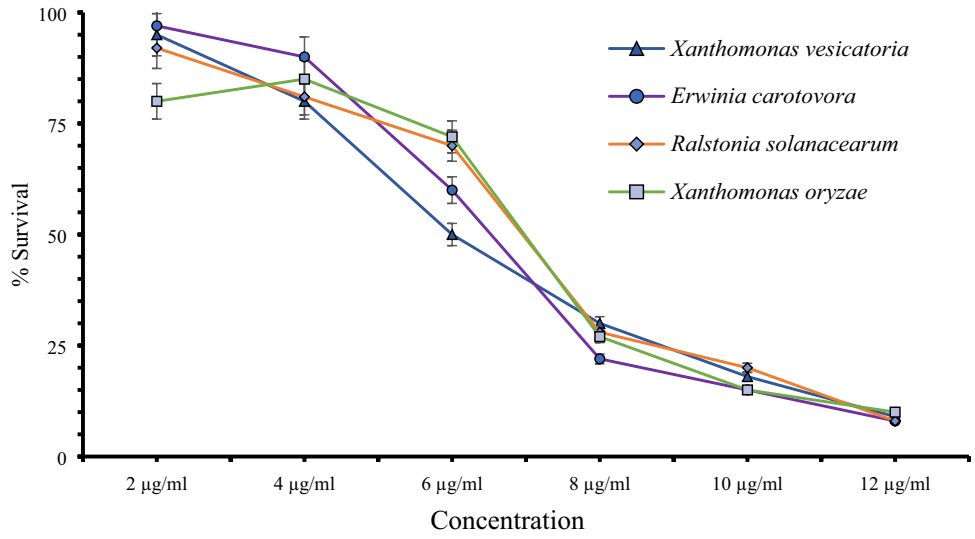

Fig. 7 Dose-dependent response of AgNPs against plant bacterial pathogens. 12 µg/ml was recorded as the MIC

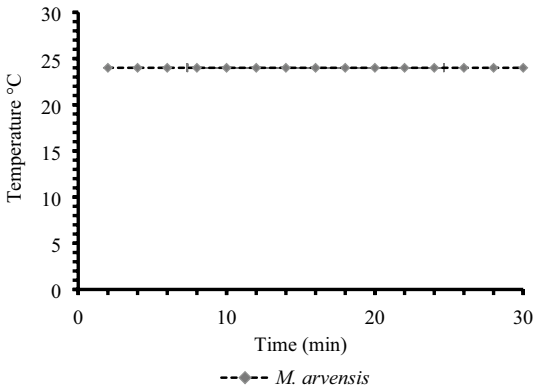

Fig. 8 Photothermal activity of AgNPs. Straight line showing no change in temperature of AgNPs even after 30 min exposure to sunlight

also interact with subcellular organelles such as mitochondria that eventually leads to cell death (Huang et al. 2011).

The generation of free radicals performs a significant job to build the cytotoxic capacity of pharmaceutical medications. A past report (Nadhman et al. 2015) proposed a direct relationship of the ROS generation with the cytotoxic potential of the oxidative-nanoparticles but our outcomes communicated zero quantum yield. Our results are indicating that ROS is not the only factor behind the cytotoxic capacities of the nanoparticles and there is no immediate or direct relationship in the generation of ROS and cytotoxic abilities in terms of non-oxidative nanoparticles. EDX investigation of the AgNPs additionally affirmed that there is no elemental O_2. Change in temperature of the NPs containing test sample is accounted for if NPs have O_2 in them. Temperature additionally plays a particularly significant role to utilize NPs as a photothermal agent to treat disease such as Leishmaniasis (Jiang et al. 2020) so the outcomes of our investigation indicated that AgNPs synthesized from *M. arvensis* cannot be utilized as a photodynamic agents in the photothermal treatment of diseases but they have a very strong potential to eradicate the population of *Leishmania* and plant bacterial pathogens due to their small size and biochemical nature.

Conclusion

Our findings explain the use of plant aqueous extract from *Mentha arvensis* for the synthesis of silver nanoparticles by the reduction of bulk silver. Biocompatible nature of silver nanoparticles favors their human applications though they are highly effective and efficacious against *Leishmania tropica* and plant bacterial pathogens. Photooxidative and photothermal analysis revealed that the non-oxidative silver nanoparticles do not have the potential to be used as photodynamic agents. This study provides experimental evidence to use NPs from *M. arvensis* to develop efficacious antimicrobial drugs to selectively target *Leishmania* and plant bacterial pathogens. Future perspectives of this work include understanding the effects of different physicochemical reaction parameters on nanoparticle corona and carving nanoparticles with different surface ligands for their targeted delivery to infected sites for photodynamic therapies.

Acknowledgements We are very thankful to the Higher Education Commission of Pakistan's, International Research Support Initiative Program (IRSIP), to send BJ to the University of Pennsylvania for experimentation. We thank Dr. Zahra Fakhraai and Aixi Zhang (Department of Chemistry, University of Pennsylvania) to support with AFM and Dr. Jamie Ford (Staff Scientist, Singh Center, University of Pennsylvania) helped with SEM facility. Authors are thankful to Dr. Abdullah Sarwer (MBBS) for explaining the phenomenon of Chloride Shift.

Author contributions ZRM and BJ devised the study. BJ performed experiments and wrote the manuscript. NIR and AN reviewed the manuscript. ZRM provided collaboration and have managed resources for the work. All the authors read and finalized the manuscript for submission.

Compliance with ethical standards

Conflict of interest The authors declare that they have no conflict of interest.

Ethics approval Hemolysis assays were performed after ethical approval from the University Bioethical Committee.

References

Abbasi BA, Iqbal J, Mahmood T et al (2019) Biofabrication of iron oxide nanoparticles by leaf extract of Rhamnus virgata: characterization and evaluation of cytotoxic, antimicrobial and antioxidant potentials. Appl Organomet Chem 33:1–15. https://doi.org/10.1002/aoc.4947

Akhtar MS, Panwar J, Yun YS (2013) Biogenic synthesis of metallic nanoparticles by plant extracts. ACS Sustain Chem Eng 1:591–602. https://doi.org/10.1021/sc300118u

Alavi M, Karimi N, Valadbeigi T (2019) Antibacterial, antibiofilm, antiquorum sensing, antimotility, and antioxidant activities of green fabricated Ag, Cu, TiO_2, ZnO, and Fe_3O_4 NPs via *Protoparmeliopsis muralis* Lichen aqueous extract against multidrug-resistant bacteria. ACS Biomater Sci Eng 5:4228–4243. https://doi.org/10.1021/acsbiomaterials.9b00274

Ali M, Kim B, Belfield KD et al (2016) Green synthesis and characterization of silver nanoparticles using *Artemisia absinthium* aqueous extract—a comprehensive study. Mater Sci Eng C 58:359–365. https://doi.org/10.1016/j.msec.2015.08.045

Alsammarraie FK, Wang W, Zhou P et al (2018) Green synthesis of silver nanoparticles using turmeric extracts and investigation of their antibacterial activities. Colloids Surf B Biointerfaces 171:398–405. https://doi.org/10.1016/j.colsurfb.2018.07.059

Alshehri MA, Aziz AT, Trivedi S et al (2019) One-step synthesis of ag nanoparticles using aqueous extracts from sundarbans mangroves revealed high toxicity on major mosquito vectors and microbial pathogens. J Clust Sci 31:177–184. https://doi.org/10.1007/s10876-019-01631-7

Anandan M, Poorani G, Boomi P et al (2019) Green synthesis of anisotropic silver nanoparticles from the aqueous leaf extract of *Dodonaea viscosa* with their antibacterial and anticancer activities. Process Biochem 80:80–88. https://doi.org/10.1016/j.procbio.2019.02.014

Bai J, Choi SH, Ponciano G et al (2000) *Xanthomonas oryzae* pv. oryzae avirulence genes contribute differently and specifically to pathogen aggressiveness. Mol Plant Microbe Interact 13:1322–1329. https://doi.org/10.1094/MPMI.2000.13.12.1322

Beddoes CM, Case CP, Briscoe WH (2015) Understanding nanoparticle cellular entry: a physicochemical perspective. Adv Colloids Interface Sci 218:48–68

Behravan M, Hossein Panahi A, Naghizadeh A et al (2019) Facile green synthesis of silver nanoparticles using *Berberis vulgaris* leaf and root aqueous extract and its antibacterial activity. Int J Biol Macromol 124:148–154. https://doi.org/10.1016/j.ijbiomac.2018.11.101

Beik J, Khateri M, Khosravi Z et al (2019) Gold nanoparticles in combinatorial cancer therapy strategies. Coord Chem Rev 387:299–324

Champoiseau PG, Jones JB, Allen C (2009) *Ralstonia solanacearum* race 3 biovar 2 causes tropical losses and temperate anxieties. Plant Heal Prog 10:35. https://doi.org/10.1094/php-2009-0313-01-rv

Ciardi JA, Tieman DM, Lund ST et al (2000) Response to *Xanthomonas campestris* pv. vesicatoria in tomato involves regulation of ethylene receptor gene expression. Plant Physiol 123:81–92. https://doi.org/10.1104/pp.123.1.81

Dembitsky VM (2002) Chlorine-containing sesquiterpenes of higher plants. Chem Sustain Dev 10:363–370

Dong YH, Zhang XF, Xu JL, Zhang LH (2004) Insecticidal *Bacillus thuringiensis* silences *Erwinia carotovora* virulence by a new form of microbial antagonism, signal interference. Appl Environ Microbiol 70:954–960. https://doi.org/10.1128/AEM.70.2.954-960.2004

Du J, Tang J, Xu S et al (2018) A review on silver nanoparticles-induced ecotoxicity and the underlying toxicity mechanisms. Regul Toxicol Pharmacol 98:231–239

Gobbo-Neto L, Bauermeister A, Sakamoto HT et al (2017) Spatial and temporal variations in secondary metabolites content of the Brazilian arnica leaves (*Lychnophora ericoides* Mart., Asteraceae). J Braz Chem Soc 28:2382–2390. https://doi.org/10.21577/0103-5053.20170092

Gottardi W, Nagl M (2005) Chlorine covers on living bacteria: the initial step in antimicrobial action of active chlorine compounds. J Antimicrob Chemother 55:475–482. https://doi.org/10.1093/jac/dki054

He Z, Zhang Y, Feng N (2020) Cell membrane-coated nanosized active targeted drug delivery systems homing to tumor cells: a review. Mater Sci Eng C 106:1–44

Huang JG, Leshuk T, Gu FX (2011) Emerging nanomaterials for targeting subcellular organelles. Nano Today 6:478–492

Huang L, Sun Y, Mahmud S, Liu H (2019) Biological and environmental applications of silver nanoparticles synthesized using the aqueous extract of *Ginkgo biloba* leaf. J Inorg Organomet Polym Mater. https://doi.org/10.1007/s10904-019-01313-x

Iqbal G, Faisal S, Khan S et al (2019a) Photo-inactivation and efflux pump inhibition of methicillin resistant *Staphylococcus aureus* using thiolated cobalt doped ZnO nanoparticles. J Photochem Photobiol B Biol 192:141–146. https://doi.org/10.1016/j.jphotobiol.2019.01.021

Iqbal J, Abbasi BA, Mahmood T et al (2019b) Green synthesis and characterizations of nickel oxide nanoparticles using leaf extract of *Rhamnus virgata* and their potential biological applications. Appl Organomet Chem 33:1–16. https://doi.org/10.1002/aoc.4950

Jadhav K, Deore S, Dhamecha D et al (2018) Phytosynthesis of silver nanoparticles: characterization, biocompatibility studies, and anticancer activity. ACS Biomater Sci Eng 4:892–899. https://doi.org/10.1021/acsbiomaterials.7b00707

Jemilugba OT, Sakho EHM, Parani S et al (2019) Green synthesis of silver nanoparticles using *Combretum erythrophyllum* leaves and its antibacterial activities. Colloids Interface Sci Commun 31:100191. https://doi.org/10.1016/j.colcom.2019.100191

Jiang X, Fan X, Xu W et al (2020) Biosynthesis of bimetallic Au–Ag nanoparticles using *Escherichia coli* and its biomedical applications. ACS Biomater Sci Eng 6:680–689. https://doi.org/10.1021/acsbiomaterials.9b01297

Khatami M, Sharifi I, Nobre MAL et al (2018) Waste-grass-mediated green synthesis of silver nanoparticles and evaluation of their anticancer, antifungal and antibacterial activity. Green Chem Lett Rev 11:125–134. https://doi.org/10.1080/17518253.2018.1444797

Kim J, Pitts B, Stewart PS et al (2008) Comparison of the antimicrobial effects of chlorine, silver ion, and tobramycin on biofilm. Antimicrob Agents Chemother 52:1446–1453. https://doi.org/10.1128/AAC.00054-07

Kim DY, Saratale RG, Shinde S et al (2016) Green synthesis of silver nanoparticles using *Laminaria japonica* extract: characterization and seedling growth assessment. J Clean Prod 172:2910–2918. https://doi.org/10.1016/j.jclepro.2017.11.123

Lamch Ł, Pucek A, Kulbacka J et al (2018) Recent progress in the engineering of multifunctional colloidal nanoparticles for enhanced photodynamic therapy and bioimaging. Adv Colloid Interface Sci 261:62–81

Li Y, Ke Y, Zou H et al (2019) Gold nano particles synthesized from Strychni semen and its anticancer activity in cholangiocarcinoma cell (KMCH-1). Artif Cells Nanomed Biotechnol 47:1610–1616. https://doi.org/10.1080/21691401.2019.1594860

Manosalva N, Tortella G, Cristina Diez M et al (2019) Green synthesis of silver nanoparticles: effect of synthesis reaction parameters on antimicrobial activity. World J Microbiol Biotechnol. https://doi.org/10.1007/s11274-019-2664-3

Nadhman A, Nazir S, Ihsanullah Khan M et al (2014) PEGylated silver doped zinc oxide nanoparticles as novel photosensitizers for photodynamic therapy against *Leishmania*. Free Radic Biol Med 77:230–238. https://doi.org/10.1016/j.freeradbiomed.2014.09.005

Nadhman A, Nazir S, Khan MI et al (2015) Visible-light-responsive ZnCuO nanoparticles: benign photodynamic killers of infectious protozoans. Int J Nanomed 10:6891–6903. https://doi.org/10.2147/IJN.S91666

Naz S, Sirajuddin M, Hussain I et al (2020) 2-Phenylbutyric acid based organotin(IV) carboxylates; synthesis, spectroscopic characterization, antibacterial action against plant pathogens and in vitro hemolysis. J Mol Struct 1203:127378. https://doi.org/10.1016/j.molstruc.2019.127378

Nindawat S, Agrawal V (2019) Fabrication of silver nanoparticles using *Arnebia hispidissima* (Lehm.) A. DC. root extract and unravelling their potential biomedical applications. Artif Cells Nanomed Biotechnol 47:166–180. https://doi.org/10.1080/21691401.2018.1548469

Odlaug TE (1981) Antimicrobial activity of halogens. J Food Prot 44:608–613. https://doi.org/10.4315/0362-028x-44.8.608

Pareek V, Gupta R, Panwar J (2018) Do physico-chemical properties of silver nanoparticles decide their interaction with biological media and bactericidal action? A review. Mater Sci Eng C 90:739–749

Parthiban E, Manivannan N, Ramanibai R, Mathivanan N (2019) Green synthesis of silver-nanoparticles from *Annona reticulata* leaves aqueous extract and its mosquito larvicidal and anti-microbial activity on human pathogens. Biotechnol Rep. https://doi.org/10.1016/j.btre.2018.e00297

Rai M, Ingle AP, Pandit R et al (2017) Broadening the spectrum of small-molecule antibacterials by metallic nanoparticles to overcome microbial resistance. Int J Pharm 532:139–148

Satsangi N (2019) Synthesis and characterization of biocompatible silver nanoparticles for anticancer application. J Inorg Organomet Polym Mater. https://doi.org/10.1007/s10904-019-01372-0

Shaiq Ali M, Saleem M, Ahmad W et al (2002) A chlorinated monoterpene ketone, acylated β-sitosterol glycosides and a flavanone glycoside from *Mentha longifolia* (Lamiaceae). Phytochemistry 59:889–895. https://doi.org/10.1016/S0031-9422(01)00490-3

Sharma VK, Yngard RA, Lin Y (2009) Silver nanoparticles: green synthesis and their antimicrobial activities. Adv Colloid Interface Sci 145:83–96

Siddiqui MN, Redhwi HH, Achilias DS et al (2018) Green synthesis of silver nanoparticles and study of their antimicrobial properties. J Polym Environ 26:423–433. https://doi.org/10.1007/s10924-017-0962-0

Thirumagal N, Jeyakumari AP (2019) Structural, optical and antibacterial properties of green synthesized silver nanoparticles (AgNPs) using *Justicia adhatoda* L. Leaf Extract J Clust Sci 31:487–497. https://doi.org/10.1007/s10876-019-01663-z

Ulaeto SB, Mathew GM, Pancrecious JK et al (2019) Biogenic Ag nanoparticles from neem extract: their structural evaluation and antimicrobial effects against *Pseudomonas nitroreducens* and *Aspergillus unguis* (NII 08123). ACS Biomater Sci Eng 6:235–245

Westen EA, Prange HD (2003) A reexamination of the mechanisms underlying the arteriovenous chloride shift. Physiol Biochem Zool 76:603–614. https://doi.org/10.1086/380208